Mansoura Engineering Journal

Volume 31 | Issue 4 Article 14

10-10-2021

Heat and Mass Transfer from Moist Air Flowing inside Cold Horizontal Circular Duct II- Experimental Study.

Hesham Mostafa
Mechanical Engineering Department., Higher Technological Institute., Tenth of Ramadan City., Egypt.,
drheshammostafa@yahoo.com

Mohamed Saafan
Mechanical Power Engineering., Faculty of Engineering., El-Mansoura University., Mansoura ., Egypt.,
mgmousa@mans.edu.eg

Recommended Citation
Mostafa, Hesham and Saafan, Mohamed (2021) "Heat and Mass Transfer from Moist Air Flowing inside Cold Horizontal Circular Duct II- Experimental Study.," *Mansoura Engineering Journal*: Vol. 31 : Iss. 4 , Article 14.
Available at: https://doi.org/10.21608/bfemu.2021.198863

HEAT AND MASS TRANSFER FROM MOIST AIR FLOWING INSIDE COLD HORIZONATL CIRCULAR DUCT II- EXPERIMENTAL STUDY

إنتقال الحرارة والكتلة من هواء رطب يمر داخل مجرى دائرى أفقى بارد II - دراسة معملية

Hesham M. Mostafa[1] and M.G. Mousa[2]

1: Higher Technological Institute, Tenth of Ramadan City, Egypt.

2: Mech. Power Eng. Dept., Faculty of Engineering, Mansoura University, Mansoura, Egypt.

Email :Mgmousa@mans.edu.eg ,DrHeshamMostafa@yahoo.com

خلاصة البحث:

فى هذا البحث تم عمل دراسة معملية لإنتقال الحرارة والكتلة الأنيين لسريان هواء رطب يمر داخل مجرى دائـرى أفقى سطحه الخارجى مبرد ومتصل بنفق هوائى. لإتمام هذه الدراسة المعملية تم تصميم وتنفيذ دائرة إختبار تتكون من نفق هوائى يتم سحب الهواء من الوسط المحيط ليمر داخل مقطع الإختبار وهو عبارة عن مجرى دائرى أفقـى قطـره ٢٥٠ مم وطوله ١٢٠٠ مم. السطح الخارجى لمقطع الإختبار يتم تبريده عن طريق إستخدام وحدتى تبريد منفصـلتين. المبخر فى كلا وحدتى التبريد عبارة عن ماسورة من النحاس الأحمر ملفوفة حول السطح الخارجى لمقطع الإختبار فى إتجاهين مختلفين وذلك للحصول على درجة حرارة ثابتة تقريبا على طول مقطع الإختبار. نتيجـة لإنخفـاض درجـة حرارة سطح مقطع الإختبار عن درجة حرارة الندى للهواء الرطب المار عليه فإن جزء من بخار الماء الموجود فـى الهواء الرطب يتم تكثيفه على السطح البارد ويتم تجميع المتكاثف فى أسفل المجرى. تم تغييرمعدل تدفق الهواء الرطب خلال التجارب وكذلك درجة حرارة السطح الخارجى لمقطع الإختبار. وقد تم قياس كل من درجات الحرارة الجافـة والندى والرطوبة النسبية والسرعة للهواء الرطب فى أماكن مختلفة على طول مقطع الإختبار وكذلك معـدل التكثيـف لبخار الماء المتجمع فى أسفل المجرى أثناء كل تجربة. وقد أجريت التجارب عند قيم مختلفة لرقم رينولـدز تتـراوح مابين ١٠٠٠ حتى ١١٠٠٠ لسريان هواء رطب وتم حساب معامل إنتقال الحرارة والكتلة وكذلك رقم نوسـلت ورقـم شيروود.

وقد أظهرت النتائج أن كمية الحرارة والكتلة المنتقلة وبالتالى رقم نوسلت ورقم شيروود يزيد مع زيادة رقم رينولـدز حتى تصل إلى أعلى قيم لهما عندما يكون رقم رينولدز حوالى ٧٠٠٠ بعدها تقل قيم رقم نوسلت ورقم شيروود نتيجـة لأن الهواء المار يحمل معه بعض من قطرات الماء المتكثفة. وبمقارنة النتائج المعملية للبحث مع النتائج مـن أبحـاث أخرى كانت نتيجة هذه المقارنة مرضية. وقد تم إستنتاج معادلتين لابعديتين لرقم نوسلت كعلاقة فى رقم رينولدز ورقم براندتل وأخرى لرقم شيروود كعلاقة فى رقم رينولدز ورقم شميدت.

Abstract

Heat and mass transfer from moist air flowing inside cold horizontal circular duct is investigated, experimentally. To perform the experimental study air tunnel is designed and manufactured. The cold horizontal circular duct (test section) is attached to the air tunnel. Moist air is drawn from the surroundings to flow inside the circular duct (250 mm in diameter and 1200 mm long). The evaporator for two separate refrigeration units is made from copper tubes. These copper tubes are warped in counter current around the outer surface of the duct to cool its surface, control and adjust the surface temperature of the duct to the desired value. According to the temperature difference between cold duct surface temperature and the dew-point temperature for the moist air flowing inside it, some of the water vapor from the moist air is condensed. Moist air flow rate and the surface temperature for the test section are controlled and adjusted during the experiments. The amount of condensate through each experiment is measured. Velocity, relative humidity, dry bulb and dew-point temperatures for moist air are taken at different positions along the test section. Reynolds number varies from 1000 to 11000. Heat and mass transfer coefficients are calculated and in turn Nusselt and Sherwood numbers are obtained.

Experimental results show that, Nusselt and Sherwood numbers increase with increasing Reynolds number up to a certain value. These increase were found due to the migration of

Accepted November 20, 2006

water bubbles with the moist air. Also, results show that heat transfer coefficient decreases with increase of wall temperature, mass transfer coefficient increases with increase of wall temperature. Comparison between the obtained experimental results and the previous works show good agreement. Two empirical correlations for Nusselt and Sherwood numbers are obtained as functions of Reynolds number and other operating parameters.

Keywords: Heat and mass transfer, moist air and Horizontal circular duct.

NOMENCLATURE

A	Surface area	m^2
A_a	Surface area of the consider segment	m^2
A_c	Cross section area	m^2
C	Concentration of water vapor in the flowing air	kg/m^3
Cp	Specific heat at constant pressure	J/(kg.K)
D	Diffusion coefficient	m^2/s
h	Heat transfer coefficient	W/(m^2.K)
h_m	Mass transfer coefficient	m/s
i	Enthalpy	J/kg
k	Thermal conductivity	W/(m. K)
L	Duct length	m
m_{air}	airflow rate	kg/s
m_v	Condensate flow rate	kg/s
m"	Mass flux	$Kg/m^2 s$
Nu	Nusselt number, (Nu=h.ro/k)	--
P	Pressure	Pa
Pr	Prandtl number, (Pr= Cp μ /k)	---
Q	Rate of heat transfer	W
q"	Heat flux	W/m^2
r_o	Duct radius	m
Re	Reynolds number , (Re = u_{av} ro/v)	---
RH	Relative humidity	%
Sc	Schmidt number, Sc=v /D	---
Sh	Sherwood number, (Sh=h_m ro/D),	--
T	Temperature	K
u_{av}	Average air velocity,	m/s
Z	Dimensionless longitudinal distance, Z=L/r_o	-

Greek symbols

ΔT	Temperature difference,	K
v	Kinematic viscosity	m^2/s
ρ	Density	kg/m^3
ω	Humidity ratio	$kg_v/kg_{dry\ air}$

Subscripts

av	Average
db	dry bulb
sat	Saturation
w	Wall
∞	Free stream

1. INTRODUCTION

Condensation process from moist air, which including heat and mass transfer has many important engineering applications, such as air conditioning applications and recovery of water from moist air. Condensation of water vapor from moist air is widely employed in heat

exchanger devices such as refrigeration units, food industries, petroleum refinery and desalination units.

Yun et al. (2006) studied, measured and analyzed the effect of surface roughness, tube material, tube thickness, and wall sub cooling on the laminar film wise condensation heat transfer coefficient on horizontal tubes at low heat transfer rates. The condensation heat transfer coefficient was significantly lower than that estimated by the Nusselt analysis when the ratio of the condensate liquid film thickness to the surface roughness was relatively low. When the condensate liquid film was very thin, tube material affected the condensation heat transfer coefficient in the film wise condensation. Therefore, the condensation heat transfer coefficients of the copper tube were higher than those of the stainless steel tubes even though they had similar surface roughness.

Jenny Lindblom and Bo Nordell, (2006) studied the condensation irrigation (CI) which is a combined system for desalination and irrigation. By evaporating seawater in, for example, solar stills and letting the humidified air transport the formed vapour into an underground pipe system, fresh water will precipitate as the air is cooled by the ground. By using drainage pipes for underground air transportation, perforations in the pipes enable the water to percolate into the soil. This study of CI focuses on the transport of humid air inside buried plain pipes, where the condensed water stays inside the pipe and may thus be collected at the pipe endings and used for drinking. Numerical simulations of this system result in a mean water production capacity of 1.8 kg/m and day over a 50-m long pipe in a diurnally steady system, though shorter pipes result in a higher mean production. A performed theoretical analysis also indicates that CI is a promising alternative irrigation method as it enables the use of saline water for irrigation

Pirompugd, W. (2005), studied and proposed a new method to calculate the heat and mass transfer characteristics of the wavy fin-and-tube heat exchangers under dehumidifying conditions. For fully wet conditions, the sensible heat transfer and mass transfer characteristics are relatively insensitive to the inlet relative humidity. The heat and mass transfer performances show appreciable influence of fin spacing at 1-row configuration. Both the heat and mass transfer performances increase when the fin spacing is reduced.

Pashitskii et al, (2004) studied a new mechanism of the hydrodynamic vortex formation in the open many-component and multi-phased systems with possible phase transitions. Consider the non-stationary solutions of the hydrodynamic equations for a vortex in the incompressible viscous medium with a substance and with unbounded inflow of substance from the exterior medium.

Novikov et al. (2004) performed an experimental study for heat and mass transfer during droplet condensation of water vapor from humid air in narrow rectangular channels. Brdlik et al. (2004) presented an experimental investigation of the heat and mass transfer accompanying condensation of water vapor from vapor-air mixtures with low volumetric vapor contents. Empirical formulas are proposed for the heat transfer coefficient and the rate of condensation.

Wang and Hihara (2003) studied new method, equivalent dry-bulb temperature (EDT) method, for calculating the cooling capacity and predicting the cooling modes of moist air over the air coil surface under partially wet and totally wet conditions. With this method, a numeric model is developed, and validated with the experimental data of plain fin air coils. The simulation deviations in cooling capacity and vapor condensate are within the range of ±10%, and the prediction for the cooling mode over the coil surfaces is fairly exact. In addition, the simulation results for plain fin air coils suggest that the heat transfer and dehumidification of the air coils under partially and totally wet-fin surface conditions can be predicted by the sensible heat transfer coefficient under the dry-fin surface condition.

Haji and Chow (1988) studied heat and mass transfer with dehumidification in laminar boundary layer flow along a cooled flat plate. The effects of dehumidification, from laminar flow humid air, over isothermal cooled flat plate have been investigated using the

similarity principle. The results obtained for both saturated and unsaturated humid air is compared with those of dry air. It can be concluded that dehumidification has a significant effect of both sensible and latent heat transfer as well as the friction factor. However, the difference in heat transfer coefficient of humid and dry air is reduced as the relative humidity is decreased.

The condensation of water vapor from moist air which including heat and mass transfer has little attention and seems to need more efforts seeking for good understanding of this process. In the present work the effect of moist air flow rate and the surface temperature of the horizontal duct on heat and mass transfer coefficients have been studied experimentally.

2. Experimental Test Rig

separate refrigeration units and measuring instruments. The main details of the test rig are presented in Fig.(1). The test section is attached to air tunnel, which provides moist air from the surroundings at different flow rates. The moist air is drawn into the air tunnel by an axial fan, which is driven by a variable speed electric motor. In accordance, the mass flow rate of moist air can be varied using the speed regulator (motor control).

The test section is a circular horizontal duct with 250 mm in diameter and 1200 mm long. The outer surface of the duct is cooled by using two separate refrigeration units (5). The evaporator for each refrigeration unit is manufacturing from copper tubes. These copper tubes for each one are warped in counter current around the outer surface of the duct to cool its surface, control and adjust the surface temperature of the duct to the desired

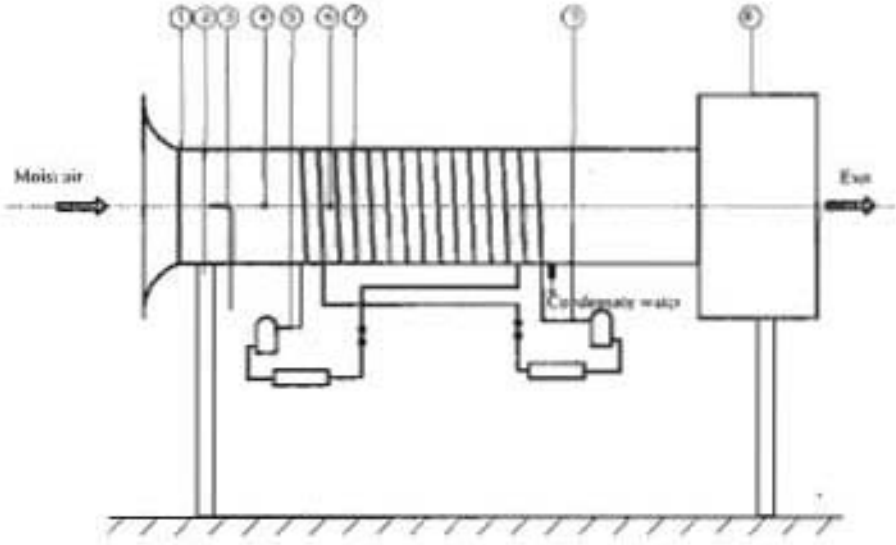

Fig. (1) Schematic diagram for the experimental test rig

1. Inlet section
2. Stand
3. Pitot tube
4. Hygrometer
5. Refrigeration Unit
6. Temperature sensor
7. Copper coil
8. Variable speed motor

The experimental test rig is designed and constructed, such that one can investigate the effect of the operating parameters of condensation process for water vapor from moist air flowing inside horizontal cold circular duct. The test rig consists mainly of horizontal circular duct (test section), air tunnel, two

value. Accordingly the difference between cold duct surface temperature and the dew-point temperature for the moist air flowing inside it, some of the water vapor from the moist air is condensed. Moist air flow rate and the temperature difference between dew-point temperature and surface temperature for the

moist air are controlled and adjusted during the experiments.

3. Experimental Measurements

Velocity, relative humidity, dry bulb and dew-point temperatures for moist air are measured at different positions along the test section. The amount of condensate through each experiment is measured.

Thermocouples, copper constantan are used to measure the surface duct temperature. All thermocouples are connected to a digital temperature recorder, which has an accuracy of ± 0.1°C. The steady state condition is achieved after a time varied from 60 to 90 minutes, depending on the value of air flow rate.

Moist air velocity measured by using Pitot tube at duct center line and at four points along the radius of the duct (at duct radius 25, 50, 75, and 100 mm). These measurements for velocity can be repeated at four sections along the duct (at distance 0.0, 400, 800, and 1200 mm from duct inlet). Then, the average value for velocity along the test section can be calculated and the corresponding value for the average value for mass flow rate of the moist air can also be obtained. In turn the corresponding frequency of motor can be recorded in Hz. By this calibration technique the mass flow rate of moist air can be varied and controlled using the motor speed regulator.

The surface temperature for the duct is measured at four points on the duct circumference (at angles 0.0, 90, 180, 270). Also, these measurements are repeated at five points along the test section (at distance 0.0, 300, 600, 900, and 1200 mm from duct inlet).

The test section is treated as four segments. Also, five slots with diameter of 12 mm and equally spaces at locations; 0.0, 300, 600, 900, and 1200 mm from duct inlet are cut in the center line of the duct. The digital hygrometer is free to move in r-direction, to ensure the possibility of measuring the relative humidity and temperature at different positions along the test section radii. The hygrometer sensor (type Testo 605-H1, with a resolution of 0.1 °C and accuracy of ±0.5 °C for temperature and a resolution of 0.1% and accuracy of ±3% for relative humidity) is mounted through these slots. The hygrometer probe diameter is of 12 mm and length 125 mm, the full scale rang for temperature from -20 to 50 °C and relative humidity up to 95%. The hygrometer is used to measure the relative humidity (RH) at different radii inside the duct (at duct radius 25, 50, 75, 100, and 125 mm). Also, the dry bulb and dew-point temperatures are measured by the same sensor.

The amount of condensate was small then it measured by using a calibrated tank and stop watch.

In order to obtain a measure of the reliability of the experimental data an uncertainty analysis was performed for the principle parameters of interest. The root-mean-square random error propagation analysis is carried out in the standard fashion using uncertainties of the basic independent variables (experimentally measured). These variables are duct dimensions, temperatures, relative humidity, air velocity, mass of condensate, which used to calculate the uncertainty in Nusselt number and Sherwood numbers. The largest calculated uncertainties in the current investigation were less than 4.5% for Reynolds number, 10.2% for Nusselt number and 8.9% for Sherwood number.

4. Experimental Procedure

Each run is carried out for certain fixed values of the problem parameters (velocity and surface temperature). Before starting a new run, the test rig is adjusted for leakage of air. The experimental procedure for each run can be described as; switch on the motor of air tunnel, adjust the frequency of motor speed of tunnel to obtain the desired flow rate for moist air, switch on the two refrigeration units and adjust the surface temperature to a certain value. The moist air is flowing inside the tunnel till steady state condition is reached. The steady state condition is achieved after about 60-90 minute. The following measurements are taken for each run; frequency of motor of tunnel (Hz), duct surface temperature, relative humidity for moist air, dry bulb temperature and dew-point temperature at different sections along the duct.

5. Data Reduction

By measuring the temperature at inlet and outlet of every segment of the duct and air velocity, one can evaluate the local and average values of heat and mass transfer coefficients and in turn Nusselt and Sherwood numbers.

Mass flow rate of dry air can be calculated according to the following equation:

$$\dot{m}_{air} = \rho_{air} \cdot u_{av} \cdot A_c \qquad (1)$$

Where ρ_{air} , u_{av} and A_c are density of air, average velocity of air and duct cross sectional area respectively.

The average heat and mass fluxes can be calculated at any segment of the duct as shown in Fig. (2), which lies between two successive measuring positions (along the length of test section) as;

$$q'' = \frac{\dot{m}_{air}}{A_a} \cdot \Delta i \,;$$

$$m'' = \frac{\dot{m}_{air}}{A_a} \cdot \Delta\omega \,. \qquad (2)$$

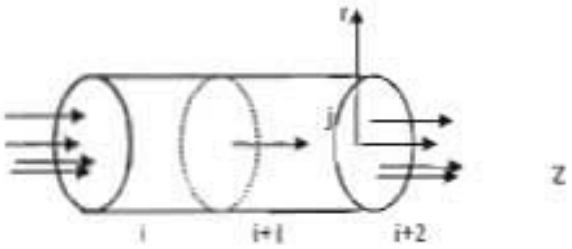

Fig.(2) Segment for calculate Heat mass transfer
Where i refer to position and j to segment

Where; q'', m'' and A_a are the heat flux, the mass flux, and the surface area of the considered segment respectively. Δi and $\Delta\omega$ are the difference of the total enthalpy and humidity ratio between the inlet and outlet of this segment. The enthalpy i and humidity ω are determined from table sited in reference [9] by knowing the average dry and dew-point temperatures at the considered section.

Accordingly, one can calculate heat and mass transfer coefficients as follows:

$$h = q''/(T_\infty - T_w),$$

$$h_m = m''/(\rho_\infty - \rho_w) \qquad (3)$$

Where; T_∞, is the dry bulb temperature for moist air far from the wall, T_w wall temperature, ρ_w density of saturated vapor at wall temperature and ρ_∞ density of superheated vapor at free stream.

One can calculate the density of superheated vapor from superheated vapor tables at dry bulb temperature, and vapor pressure P_v. the vapor pressure calculated as;

$$P_v = RH \,.P_{sat} \qquad (4)$$

Where; RH, and P_{sat} are relative humidity, and saturated vapor pressure respectively.

Accordingly, one can calculate local Reynolds, Nusselt and Sherwood numbers as:

$$Re = \frac{u_{av} \cdot r_o}{\nu}, \quad Nu = \frac{h \cdot r_o}{k}, \quad Sh = \frac{h_m \cdot r_o}{D} \qquad (5)$$

Where; r_o, ν, k and D are duct radius, kinematics viscosity, thermal conductivity of air and mass diffusion coefficient respectively.

6. Results and Discussion

In this section the obtained experimental results are presented and discussed. Accordingly, the experimental results, dry bulb and dew-point temperatures, local and average heat transfer, as well as mass transfer coefficients local and average Nusselt and Sherwood numbers are depicted. Also a comparison between the present results and that of previous available works are also presented.

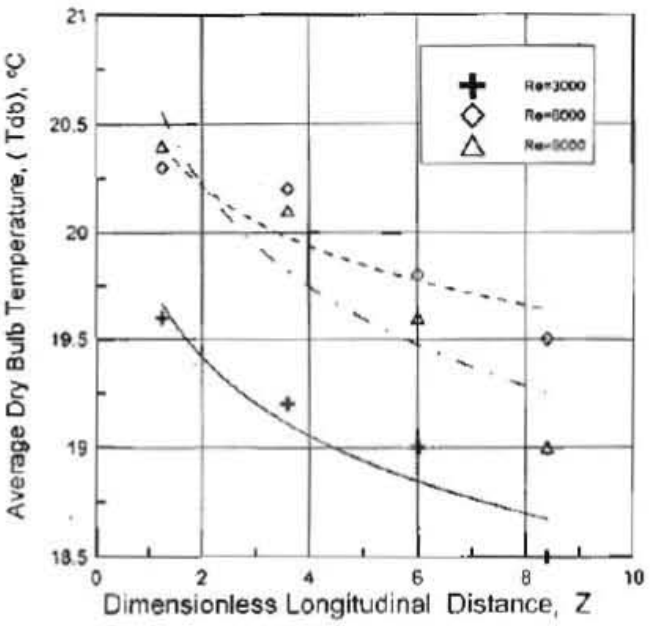

Fig.(3) Distribution of the average dry blub temperature along the dimensionless longitudinal distance at different values of Reynolds number

Dry bulb and dew-point temperatures are measured at different radii and then the average value can be calculated. This can be repeated at five positions along the duct length (i.e. at inlet and outlet of each segment). Figures (3 and 4) show samples of dry bulb and dew-point temperatures distributions versus the dimensionless longitudinal distance ($Z=L/r_o$). As shown in figures (3 and 4), dry and dew-point temperatures decrease in down stream direction.

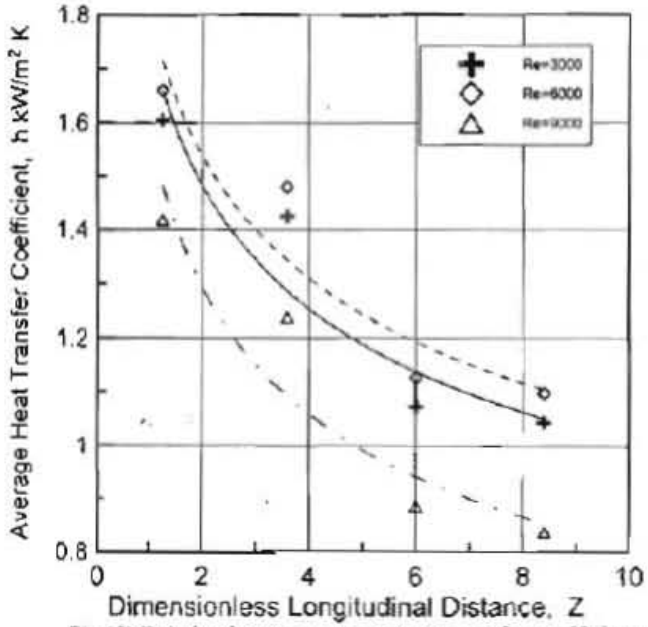

Fig.(5) Relation between average heat transfer coefficient and dimensionless distance,

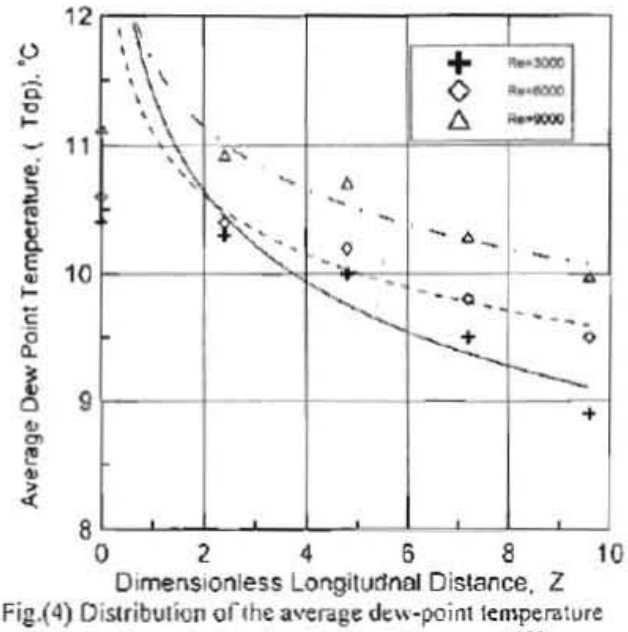

Fig.(4) Distribution of the average dew-point temperature along the dimensionless longitudinal distance at different values of Reynolds number

Figure (5) shows the variation of the averge heat transfer coefficients versus the dimensionless longitudinal distance (Z) at

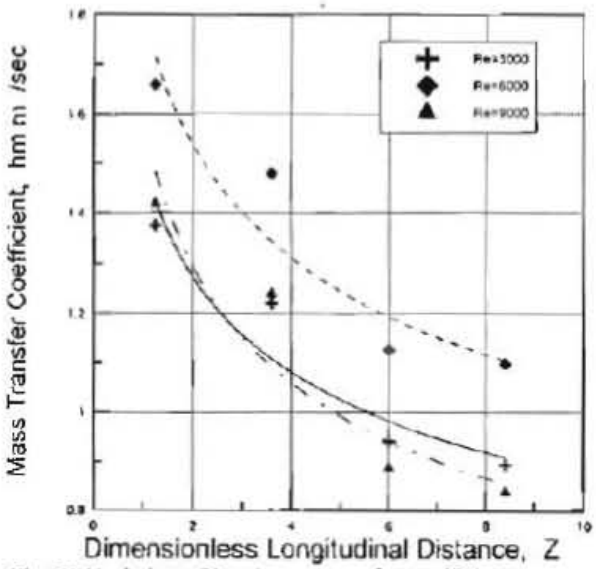

Fig.(6) Variation of local mass transfer coefficient versus dimensionless longitudinal distance.

different values of Reynolds number. It is observed that, the average values for heat transfer coefficient decrease with increasing dimensionless longitudinal distance, (Z) and increase with increasing Reynolds number from 3000 to 6000, but it decrease for increasing Reynolds number to 9000.

Also, Figure (6) shows the variation of the average mass transfer coefficients versus the dimensionless longitudinal distance at different values of Reynolds number. It takes the same trend like heat transfer coefficient.

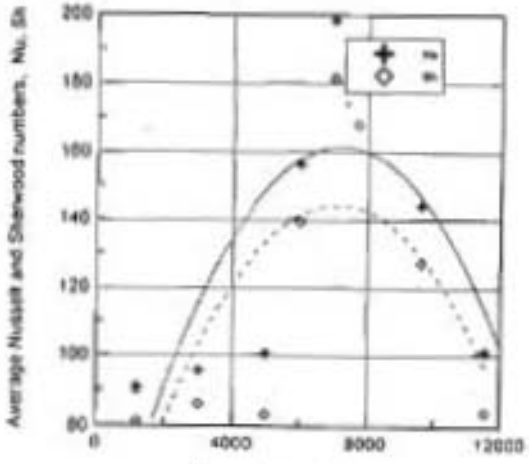

Fig.(7) Relation between Nusselt and Sherwood numbers and Reynolds number.

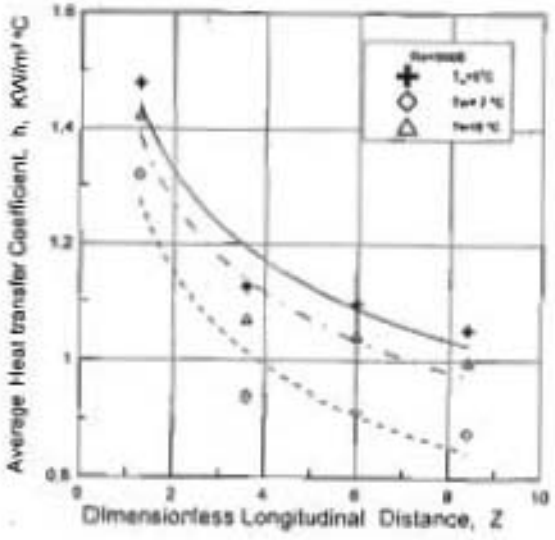

Fig.(8) Variation of Average Heat transfer coefficient versus dimensionless longitudinal distance at different wall temperature.

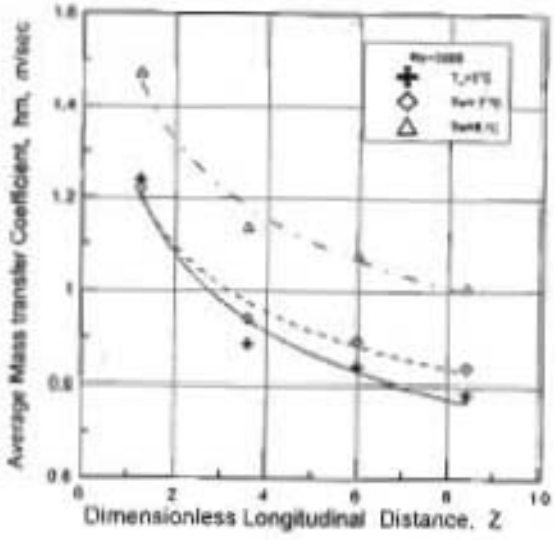

Fig.(9) Variation of Average mass transfer coefficient versus dimensionless longitudinal distance at different wall temperature

Average values for Nusselt and Sherwood numbers are plotted against Reynolds number, as shown in Fig. (7). The average Nusselt and Sherwood numbers increase with increasing Reynolds number up to about Re=7000. At this point the average Nusselt and Sherwood numbers take the maximum values and there is a peak. Then the values of the average Nusselt and Sherwood numbers decrease with increasing Reynolds number, due to the migration of the condensate water bubbles with the moist airflow. Because of this migration, the rate of condensation, and in turn, rate of heat and mass transfer are decreased.

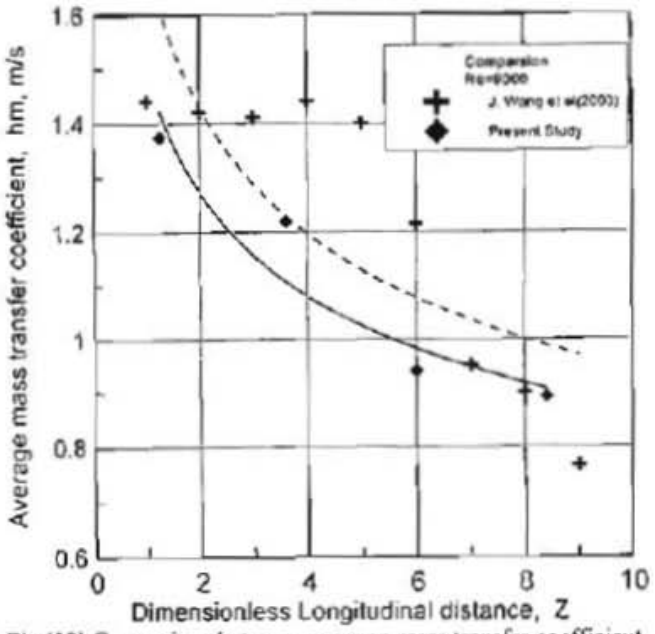

Fig.(10) Comparison between average mass transfer coefficient for the present study with the previous work.

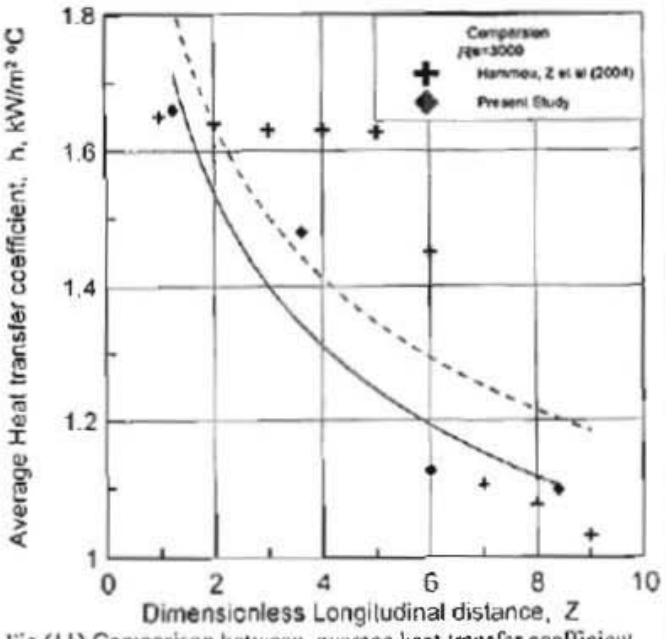

Fig.(11) Comparison between average heat transfer coefficient for the present study with the previous work

Figures (8) show the variation of the average values for heat transfer coefficient against longitudinal distance (Z), at Reynolds number equal 3000, for different values of wall temperature. The values of the average heat transfer coefficient decrease with increase the wall temperature. Figure (9) show the relation between average mass transfer coefficient and dimensionless longitudinal distance (Z) mass transfer coefficient increase with increasing wall temperature.

Figure (10) shows a comparison between the present experimental results for the local mass transfer coefficient versus dimensionless longitudinal distance, (Z) and the previous work for Wang and Hihara (2003), which cool moist air over coil surface. It is observed that, both results have the same trend.

Figure (11) shows a comparison between the present experimental results for the local heat transfer coefficient versus dimensionless longitudinal distance and the previous work for Wang and Hammou (2004). It is noticed that, both results are in good agreement.

The following relations correlate the experimental results, where the Nusselt and Sherwood numbers are expressed as functions of Reynolds, Prandtl and Schmidt numbers as;

$$Nu = 2.61\ Re^{0.64}\ Pr^{0.34}$$

$$Sh = 2.22\ Re^{0.612}\ Sc^{0.34}$$

Conclusions

In the present study, the condensation process of water vapor from moist air is, experimentally, analyzed. Experimental results show that, there is an optimum value of Reynolds number, thereafter the increase of flow velocity, and in turn, the Reynolds number cause a decrease of condensation rate, and in turn, Nusselt and Sherwood numbers. For the present operating conditions, this value of Reynolds number is found to be about 7000. The corresponding values of Nusselt and Sherwood numbers are about 200 and 180 respectively. Increasing wall temperature cause a decrease in Nusselt number and increase Sherwood number with decrease wall temperature.

Comparison between the obtained experimental results and the previous works gave good agreement. Empirical correlations for Nusselt number and Sherwood number are obtained.

REFERENCES

[1] **Yun, R., Heo, J., Kim, Y. (2006),** "Effects of surface roughness and tube materials on the film wise condensation heat transfer coefficient at low heat transfer rates" International Communications in Heat and Mass Transfer Vol. 33, pp. 445–450.

[2] **Jenny Lindblom and Bo Nordell (2006)** 'Water production by underground condensation of humid air' Desalination Volume 189, No. 1-3 , PP. 248-260

[3] **Wang, J., and Hihara, E. (2003),** "Prediction of air coil performance under partially wet and totally wet cooling conditions using equivalent dry-bulb temperature method" International Journal of Refrigeration, Vol. 26, Issue 3 ,pp. 293-301.

[4] **Hammou, Z. A., Benhamou, B., Galanis, N. and Orfi, J. (2004),** "Laminar mixed convection of humid air in a vertical channel with evaporation or condensation at the wall". Int .J. Thermal Sciences. Vol. 43. pp. 531-539.

[5] **Pashitskii, E., Anchishkin, D., Matnev, V., and Naryshkin, R. (2004).** "Possible mechanism of atmospheric vortices development under condensation of water vapor in dense cloud systems". Int .J. Thermal Sciences, Vol. 43, pp. 540-552.

[6] **Eames, I. W., Marr, N. J. and Sabir, H., (1997),** "The condensation coefficient of water : a review," Int. J. Heat and Mass Transfer, Vol. 40, No. 12, pp. 2963-2973.

[7] **Zheng, G. S. and Worek, W. M., (1996),** "Method of heat and mass transfer enhancement in film condensation" Int. J. Heat and Mass Transfer. Vol. 39, No. 1. pp. 97-108.

[8] **Haji, M. and Chow, L. C., (1988),** "Experimental measurement of water condensation rates into air and superheated steam," ASME J. Heat Transfer, Vol. 110, pp. 237-242.

[9] **Borgnakke, C. and Sonntay, R. E., (1997),** "Table of Thermodynamic and transport Properties," John Wiley & sons Inc.

[10] **Brdlik, P. M., Kozhinov, I. A., and Petrov, N. G., (2004),** "Experimental investigation of heat and mass transfer during condensation of water vapor from humid air on a vertical surface under natural convection conditions" Journal of Engineering Physics and Thermophysics, pp.164-166

[11] **Novikov, P. A., and Shcherbakov, L. A., (2004).** "Heat and mass transfer during droplet condensation of water vapor from a stream of rarefied humid air in narrow rectangular channels" Journal of Engineering Physics and Thermophysics, pp.1323-1326.